Citation &
Copyright (to be inserted by the publisher)

Crystallographic Distribution of Low Angle Grain Boundary Planes in Magnesium Oxide

D.M. Saylor[1], A. Morawiec[2], K.W. Cherry[1], F.H. Rogan[1], G.S. Rohrer[1], S. Mahadevan[3] and D. Casasent[3]

[1] Materials Science and Engineering Dept., Carnegie Mellon University, Pittsburgh, PA 15213, USA

[2] Instytut Metalurgii i Inzynierii Materialowej PAN, Reymonta 25, 30-059 Krakow, Poland

[3] Electrical and Computer Engineering Dept., Carnegie Mellon University, Pittsburgh, PA 15213, USA

Keywords: grain boundaries, misorientation, microstructure, grain boundary distribution, magnesium oxide.

Abstract. We have developed a technique that allows all five macroscopically observable grain boundary degrees of freedom to be characterized for a statistically significant number of interfaces. Using this technique, we have characterized 5 x 10^6 μm^2 of grain boundary plane area in a 0.15 mm^3 volume of MgO. The observations demonstrate that there is significant texture in the distribution of boundary planes. Here we compare the observed distribution of grain boundary planes at low misorientation angles (~ 5 °) to the calculated geometrically necessary dislocation content of the same interfaces. Based on the inverse correlation between these two quantities, we conclude that relatively low energy configurations are adopted with the highest frequency.

Introduction

There are five macroscopically observable characteristics of a grain boundary: three describe the lattice misorientation and two describe the boundary inclination [1]. While the distribution of lattice misorientations is frequently derived from the analysis of planar sections [2,3], grain boundary inclinations are rarely reported for more than a handful of boundaries. The goal of characterizing all five degrees of freedom for a statistically significant number of boundaries is complicated by the number of geometrically distinguishable configurations. For example, if one resolves the macroscopically observable parameters of grain boundaries in a cubic material with 5 ° of resolution, then there are approximately $2x10^5$ distinct configurations [4]. Therefore, the domain of distinct grain boundaries is too large to be practically sampled by traditional microscopies that require the continuous attention of a human operator.

We have developed a semi-automated technique that combines scanning electron microscope (SEM) imaging, orientation mapping, and serial sectioning to characterize all five macroscopic degrees of freedom for a statistically relevant number of grain boundaries in a polycrystalline sample. In the present paper, we describe the principles of the method and analyze the distribution of low angle grain boundaries (~ 5 ° misorientation angle). The relative frequency of occurrence of different grain boundary configurations is compared to the density of geometrically necessary dislocations required to form the interfaces. We demonstrate here that the most frequently observed boundary planes are those that can be formed with the lowest dislocation density. Assuming a correlation between the dislocation density and the energy of the interface, we conclude that the total interfacial free energy is reduced by grain boundary plane texture.

Experimental Methods

Magnesia powder was formed by decomposing 99.7% pure magnesium carbonate at 997°C in air. Uniaxial compaction in a hot press at 1700°C for one hour at 61 MPa produced a disc with a diameter of 50 mm and an average thickness of 1.5 mm. Specimens cut from this disc were then packed in a magnesia crucible with the parent powder and annealed for 48 h at 1600°C in air. Polished surfaces were thermally grooved to reveal the grain boundaries by annealing in air for 5 h at 1400°C. One of the assumptions which underpins our measurement is that all of the boundaries form detectable grooves and that the boundaries do not migrate at the grooving temperature. The average grain size of the sample was 109 μm. Impurity analysis indicated that the sample contained 0.2% Ca, 0.02% Al, 0.03% Fe, 0.02% Si, and 0.03% Y. This sample exhibited a strong <111> axial texture that was 11 times random at the maximum.

Acquisition of the geometric and crystallographic data required to characterize the five grain boundary degrees of freedom requires orientation measurements with high spatial resolution from multiple sections through the sample. This was accomplished using an automated SEM mapping system that controls both the stage and beam position so that a large number of spatially correlated images and electron backscattered diffraction patterns (EBSPs) can be recorded. When the mapping is conducted, the sample surface is initially divided into sectors. At each sector, a secondary electron image is recorded, and EBSD measurements of crystallite orientation are made at regular intervals within the sector. When the sector characterization is complete, the microscope stage is automatically moved to the next sector, which has a small overlap with the previous one. The entire procedure is carried out under computer control. Because we use SEM images to determine grain boundary positions, the orientation measurements can be conducted at relatively coarse intervals. Thus, compared to the conventional orientation imaging microscopy methods [5], we are able to resolve the boundary positions accurately without accumulating overly redundant orientation data. After an area is mapped, high precision serial sectioning is used to remove a thin layer (7 μm on average) and the process is repeated so that the three-dimensional characteristics of the grain boundary network can be determined.

To collect the microscopic data, the sample was coated with carbon and tilted to 60° in the SEM. On each layer of the sample, three 14 x 14 grids, each containing 196 sectors, were characterized. In each sector, a tilt-corrected image was taken at 750x magnification, and 300 uniformly distributed orientation measurements were recorded. As a result, the spacing between the pixels in the SEM images is 0.25 μm and the spacing between EBSPs is 8 μm. Five parallel layers were analyzed in this way.

The information in the SEM images and crystallite orientation measurements were combined to produce high-resolution orientation maps. After correcting spatial distortions in each image, the relative positions of the images in each layer were determined using the algorithm described by Mahadevan and Casasent [6]. Next, the grain boundary positions in each sector image were digitized by hand. The relative positions of images were then used to construct large mosaic maps of the grain boundaries and orientation measurements on each layer. To produce orientation maps from these data, every grain in the scan area, defined by contiguous pixels not associated with a grain boundary, was identified and assigned an orientation. Because multiple orientation measurements were made in each grain, minority orientations resulting from errors in the indexing had to be excluded. The remaining majority orientations, which contained some scatter, were averaged to make the final orientation assignment for each grain [7,8].

We established a global reference frame (based on the first layer) in the following way. The transformation from each layer to the first layer is given by $\mathbf{Ax+t}$ where $\mathbf{x}$ is a two dimensional

vector which represents the position within a given layer, **A** is a 2x2 affine transformation matrix, and **t** is a two dimensional translation vector. To find (**A**,**t**) for each layer, we initially find (**A**,**t**) that maximizes the area of overlap between positions with the same orientations on adjacent layers. We then use the (**A**,**t**) describing the transformation that aligns adjacent layers to calculate the (**A**,**t**) that aligns each layer with the initial layer.

After each layer was transformed into the global reference frame, the common grains through all the layers were identified using the following algorithm. The area of overlap between all grain pairs on adjacent layers was determined. The pair of grains that has the largest area of overlap is identified as being two sections of the same grain. The pair with the second largest area of overlap is then assigned in the same way. The process continues until all grains have been assigned or do not overlap any grains that have not been assigned. The success of this algorithm, which we have found to be 99.5% accurate, derives from the fact that the distance between adjacent layers is much smaller than the average grain size. The orientations of the crystallites were then reassigned by considering all of the orientation data from different section planes of the same grain. After the grains were identified on all layers, pixels associated with common grain boundaries on adjacent layers were used to create a meshed interfacial surface of triangular elements. The final grain boundary network consisted of 4.1×10^6 distinct triangular elements.

After all boundaries were meshed, it was possible to determine the distribution of grain boundaries over all five mesoscopically observable parameters. Using the vertices of the triangles in the mesh, the area and normal vector for each triangle were determined. Next, the normal vector and the orientations of the crystallites bounding each triangle were used to specify all five grain boundary parameters, and the total boundary area associated with each discrete grain boundary can be calculated. The space of grain boundaries is discretized in the following manner. The misorientations, each described by three Eulerian angles (ϕ_1,Φ,ϕ_2), were parameterized by ϕ_1, $\cos(\Phi)$, and ϕ_2 in the range of zero to $\pi/2$, 1, and $\pi/2$, respectively. The inclinations, described by two spherical angles, θ and ϕ, were parameterized by $\cos(\theta)$ and ϕ in the range of zero to 1 and 2π, respectively. This domain of grain boundary space was tessellated into cells by dividing the range of each parameter into twelve equal partitions, a resolution of approximately 10°, each cell representing a discrete grain boundary type. Within this domain, 36 symmetrically equivalent grain boundaries exist for each characterized grain boundary.

Results

The observed planes were not evenly distributed over the five-dimensional space of possible grain boundary configurations. If we consider the distribution of boundaries with respect to only the three misorientation parameters, a strong peak is found at low angle misorientations (~ 14 times random at maximum). The results and discussion in this paper are limited to these low misorientation angle boundaries.

To illustrate the distribution of misorientation axes for grain boundaries with a misorientation angle less than 10 °, we have plotted the relative population of boundaries with different misorientation axes in stereographic projection (see Fig. 1a). Note that the distribution peaks at <110> and that very few boundaries that have misorientations axes within 35 ° of <100> and 10 ° of <111> are observed.

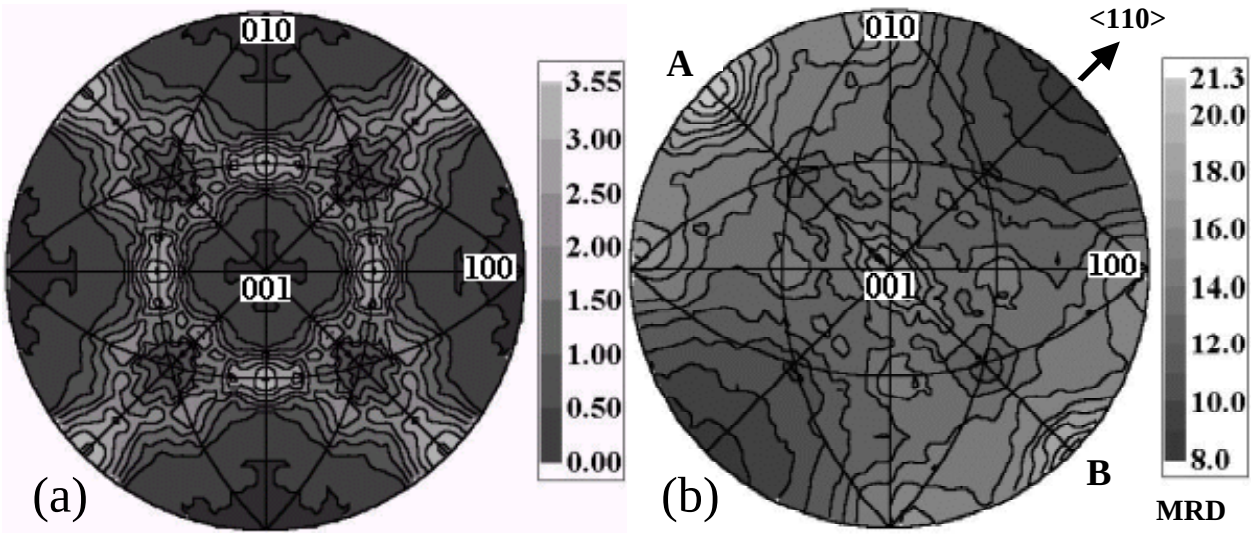

Figure 1: (a) Contour plot in stereographic projection of the distribution of misorientation axes for low angle (< 10 °) misorientations. The value of the distribution increases as the shading in the plots varies from dark to light, and the contour values are given on the scale bar. The units are in multiples of a random distribution of axes. (b) Contour plot in stereographic projection of the distribution of grain boundary planes for misorientations of 5 ° around the <110> axis.

We represent the distribution of low misorientation angle grain boundary planes by plotting the relative population of grain boundary normals in stereographic projection, as illustrated in Fig. 1b. Considering the relatively high population of boundaries with <110> misorientation axes and the fact that the discretization of the five parameter space has a resolution of about 10 °, we have selected a representative point in misorientation space corresponding to a 5 ° rotation about <110> for consideration. Note that the population of boundaries is highest along the great circle that is perpendicular to the misorientation axis. In Fig. 1b, this circle projects to the line joining the $(\bar{1}10)$ and $(1\bar{1}0)$ planes, labeled A and B, respectively. Because the misorientation axis lies in the plane of these boundaries, they have a pure tilt character. Among all of the pure tilt boundaries, there is a preference for boundaries with {110}-type planes. Note also that there is a very low population of boundaries with pure twist character (those with planes perpendicular to the misorientation axis).

Discussion

To understand the physical origin of the observed distribution of grain boundary planes, we consider the Read-Shockley [9] model, which predicts that the energies of grain boundaries with low misorientation angles will vary with the density and energy of the dislocations that compensate for the misfit. The number and type of dislocations required for a given grain boundary ultimately depends on both the misorientation and the boundary plane. Thus, by determining the dislocation densities for low angle boundaries we can estimate the relative energy variation and compare it to the observed distribution.

To calculate dislocation densities, we use Frank's formula for a general grain boundary [10]. Given the boundary character (misorientation and boundary normal) and a set of three noncoplanar Burgers vectors (b_i), the formula allows the density and orientation of the i^{th} set of dislocations (corresponding to b_i) that make up the boundary to be determined. The dislocation model, N_i, is calculated from

$$N_i = b_i^* \times u - n(n \bullet b_i^* \times u), \tag{1}$$

where u is the misorientation axis, n is the boundary plane normal, and b_i* are the reciprocal vectors given by:

$$b_1^* = \frac{b_2 \times b_3}{b_1 \bullet (b_2 \times b_3)}. \tag{2}$$

Similar relations are obtained for b_2* and b_3* by rotating subscripts. The direction of the vector N_i specifies the orientation of the i^{th} set of dislocations. The density is given by $\theta|N_i|$, where θ is the misorientation angle.

For magnesia, we have considered dislocations with $b = a/2<110>$ and $b = a/2<100>$. Therefore, there exist many possible combinations of three noncoplanar Burgers vectors and each corresponds to a different dislocation model. To find the "best" model we evaluated all possible combinations, and the one which yielded the lowest density was considered to be correct. Figure 2a shows the calculated dislocation density for a 5 ° rotation about the <110> axis. Based on these data, we observe that the density is lowest for the pure tilt boundaries and highest for the pure twist. Furthermore, the minimum dislocation density is found for boundaries on $(\bar{1}10)$ and $(1\bar{1}0)$ planes.

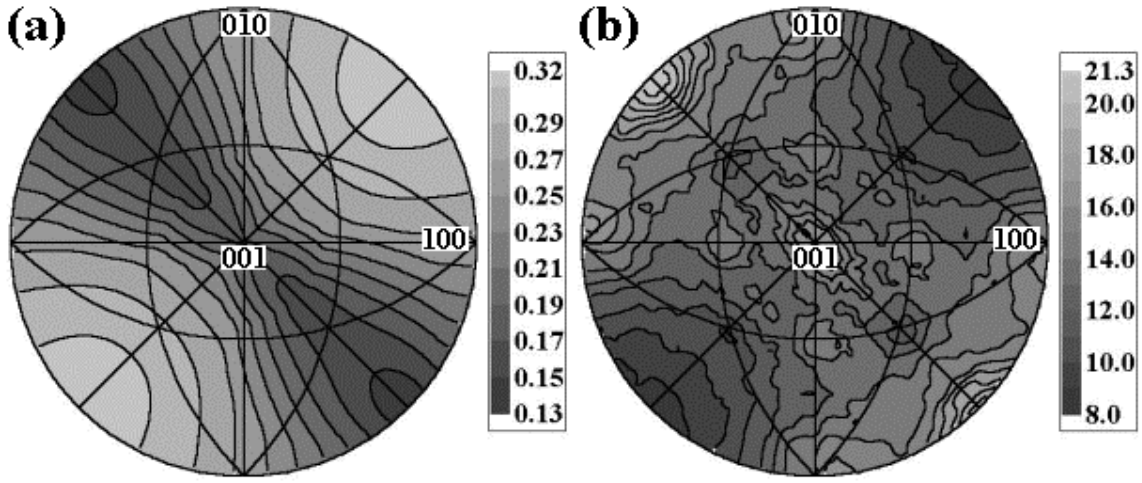

Figure 2: Calculated dislocation densities, plotted in stereographic projection for the misorientation corresponding to a 5 ° rotation about <110>, are shown in (a). The density increases as the shading in the plots varies from dark to light. The contour values are shown in the scale bar and have units of dislocations/nm^2. For reference the grain boundary character distribution for the same misorientation is shown in (b).

There is a strong inverse correlation between the geometrically necessary dislocation density and the observed distribution of interfaces. According to the Read-Shockley [9] model for low angle grain boundaries, the free energy of the per unit area of an interface plane should increase with the density of geometrically necessary dislocations. Therefore, the observed distribution of boundary

planes corresponds to a relatively low energy configuration (compared to a random distribution). Recalling that this microstructure was formed by extensive grain growth, one possible explanation for the origin of the observed distribution is that the relatively high energy boundaries are preferentially eliminated to reduce the total interfacial energy. A strong (positive) correlation between grain boundary energy and mobility would provide a mechanism for this process. Therefore, the distribution of grain boundary planes in this microstructure would be analogous to the distribution of facets on the growth form of an isolated crystal, where classical crystal growth theory predicts that the slowest moving facets have the largest relative surface area.

Summary

We have developed a technique that allows all five macroscopically observable grain boundary degrees of freedom to be characterized for a statistically significant number of interfaces. At low misorientation angles, grain boundaries planes with the smallest geometrically necessary dislocation content occur with the highest frequency, suggesting a correlation between the grain boundary energy and the grain boundary population.

Acknowledgement

This work was supported primarily by the MRSEC program of the National Science Foundation under Award Number DMR-0079996.

References

[1] C. Goux, Can. Metall. Q., 13 (1974), p. 9.

[2] J. Pospiech, K. Sztwiertnia, and F. Haessner, *Textures Microstruct.*, 6 (1986), p. 201.

[3] F. Heidelbach, H.R. Wenk, S.R. Chen, J. Pospiech, and S.I. Wright, *Mater. Sci. Engng. A*, A215, (1996), p. 39.

[4] D.M. Saylor, A. Morawiec, B.L. Adams, and G.S. Rohrer, Interface Science, 8 (2000), p. 131.

[5] B.L. Adams, S.I. Wright, and K. Kunze, Met. Trans., 24A (1993) p. 819.

[6] S. Mahadevan and D. Casasent Proceedings SPIE, Vol. 4387, (2001), p. 204.

[7] M. Humbert, N. Gey, J. Muller, and C. Esling, J. Appl. Cryst., 29 (1996), p. 662.

[8] A. Morawiec, J. Appl. Cryst., 31 (1998), p. 818.

[9] F.C. Frank, *A Symposium on the Plastic Deformation of Crystalline Solids*. Office of Naval Research, Washington, DC, 1950, p. 151.

[10] W.T. Read and W. Shockley, Phys. Rev. 78 (1950), p. 275.